JARO 15: 45–55 (2014)
DOI: 10.1007/s10162-013-0427-7

JARO
Journal of the Association for Research in Otolaryngology

Research Article

Hearing Impairment in Hypothyroid Dwarf Mice Caused by Mutations of the Thyroid Peroxidase Gene

Kenneth R. Johnson,[1] Leona H. Gagnon,[1] Chantal M. Longo-Guess,[1] Belinda S. Harris,[1] and Bo Chang[1]

[1] *The Jackson Laboratory, 600 Main Street, Bar Harbor, ME 04609, USA*

Received: 22 July 2013; Accepted: 5 November 2013; Online publication: 3 December 2013

ABSTRACT

Thyroid hormone (TH) is essential for proper cochlear development and function, and TH deficiencies cause variable hearing impairment in humans and mice. Thyroid peroxidase (TPO) catalyzes key reactions in TH synthesis, and *TPO* mutations have been found to underlie many cases of congenital hypothyroidism in human patients. In contrast, only a single mutation of the mouse TPO gene has been reported previously (Tpo^{R479C}) but was not evaluated for auditory function. Here, we describe and characterize two new mouse mutations of *Tpo* with an emphasis on their associated auditory deficits. Mice homozygous for these recessive mutations have dysplastic thyroid glands and lack detectable levels of TH. Because of the small size of mutant mice, the mutations were named teeny (symbol Tpo^{tee}) and teeny-2 Jackson ($Tpo^{tee\text{-}2J}$). Tpo^{tee} is a single base-pair missense mutation that was induced by ENU, and $Tpo^{tee\text{-}2J}$ is a 64 bp intragenic deletion that arose spontaneously. The Tpo^{tee} mutation changes the codon for a highly conserved tyrosine to asparagine (p.Y614N), and the $Tpo^{tee\text{-}2J}$ mutation deletes a splice donor site, which results in exon skipping and aberrant transcripts. Mutant mice are profoundly hearing impaired with auditory brainstem response (ABR) thresholds about 60 dB above those of non-mutant controls. The maturation of cochlear structures is delayed in mutant mice and tectorial membranes are abnormally thick. To evaluate the effect of genetic background on auditory phenotype, we produced a C3.B6-$Tpo^{tee\text{-}2J}$ congenic strain and found that ABR thresholds of mutant mice on the C3H/HeJ strain background are 10–12 dB lower than those of mutant mice on the C57BL/6 J background. The *Tpo* mutant strains described here provide new heritable mouse models of congenital hypothyroidism that will be valuable for future studies of thyroid hormones' role in auditory development and function.

Keywords: cochlear development, thyroid hormone, TPO, mouse mutation, ABR, tectorial membrane, strain background

INTRODUCTION

The auditory system is highly sensitive to the effects of thyroid hormone (TH), especially during important embryonic and neonatal periods (Deol 1973; Uziel 1986). Mouse models of hypothyroidism have been instrumental in elucidating the role of TH in cochlear development and auditory function. Auditory deficits have been described in congenitally hypothyroid mice caused by mutations that impair pituitary function with secondary effects on the thyroid, such as $Pou1f1^{dw}$ (Mustapha et al. 2009) and $Prop1^{df}$ (Fang et al. 2012); mutations that prevent normal thyroid development, such as $Pax8^{tm1Pgr}$ (Christ et al. 2004); and mutations that impede or block the synthesis of TH, such as $Tshr^{hyt}$ (O'Malley et al. 1995; Sprenkle et al., 2001), $Slc26a4^{tm1Egr}$ (Everett et al. 2001), and $Duox2^{thyd}$ (Johnson et al. 2007). Hearing loss and cochlear abnormalities also have been reported in mice with mutations that prevent peripheral responses to TH, such as mutations of the TH receptors *Thra* and *Thrb* (Rusch et al. 2001; Griffith et al. 2002; Winter et al.

Correspondence to: Kenneth R. Johnson · The Jackson Laboratory · 600 Main Street, Bar Harbor, ME 04609, USA. Telephone: +1-207-2886228; fax: +1-207-2886073; e-mail: ken.johnson@jax.org

2006) and mutations of the deiodinases *Dio2* and *Dio3* (Ng et al. 2004; Ng et al. 2008).

Thyroid peroxidase (TPO) catalyzes crucial steps in the synthesis of TH. TPO is located on the apical surface of thyroid follicular cells and catalyzes the iodination of tyrosine residues of thyroglobulin and the coupling of iodotyrosines to form the thyroid hormones T3 and T4. It therefore is essential in thyroid hormonogenesis, and its loss of function results in severe congenital hypothyroidism. Mutations of the *TPO* gene have been shown to underlie many cases of congenital hypothyroidism due to iodide organification defects in human patients, including both missense and frameshift mutations (Bakker et al. 2000; Ambrugger et al. 2001; Wu et al. 2002). Hearing impairment has been shown to be associated with some of these *TPO* mutations (Pfarr et al. 2006). In contrast to the prevalence of human *TPO* mutations, only a single mutant mouse has been reported with a *Tpo* mutation (Tpo^{R479C}), and auditory function was not evaluated in these mutant mice (Takabayashi et al. 2006).

In this study, we molecularly characterize two new independently arising recessive mutations of the mouse *Tpo* gene and analyze the mutant phenotypes associated with these mutations, with particular emphasis on auditory function. We show that the congenitally hypothyroid mutant mice are severely hearing impaired and that this impairment is associated with delayed development of cochlear structures and a dysmorphic tectorial membrane, similar to the effects seen in other mouse models of hypothyroidism. We also show that strain background influences the severity of hearing impairment in the *Tpo* mutant mice.

METHODS

Mice

Mice with the two *Tpo* mutations are publicly available from The Jackson Laboratory (http://jaxmice.jax.org/index.html); the strain carrying the *tee* mutation is designated C57BL/6J-Tpo^{tee}/GrsrJ, and the strain carrying the *tee-2J* mutation is designated B6.Cg-$Tpo^{tee\text{-}2J}$ $H2^{g7}$/GrsrJ. To investigate the effects of *Tpo* mutations on a different strain background, we generated a C3H/HeJ congenic strain containing the *tee-2J* mutation, which was derived from the B6.Cg-$Tpo^{tee\text{-}2J}$ $H2^{g7}$/J strain by repeatedly backcrossing hybrid progeny to C3H/HeJ mice and selecting for the $Tpo^{tee\text{-}2J}$ mutation at each generation until six backcross generations (N6) were completed. The resulting congenic strain, designated C3.B6-$Tpo^{tee\text{-}2J}$/Kjn, is available from the Jackson Laboratory. Experimental mice were housed in the Research Animal Facility of The Jackson Laboratory, and all procedures involving their use were approved by the institutional animal care and use committee. The Jackson Laboratory is accredited by the American Association for the Accreditation of Laboratory Animal Care.

Thyroid Gland and Inner Ear Histology

Anesthetized mice were perfused through the left ventricle of the heart with phosphate-buffered saline followed by Bouin's fixative. Thyroid glands were dissected out of the body, fixed in Bouin's for 7 days, and embedded in paraffin. Sections were cut (6-μm thick), mounted on glass slides. Thyroid tissue was counterstained with hematoxylin and eosin (H&E). Inner ears were dissected out of the skull, immersed in Bouin's fixative for 21 days, and embedded in paraffin. Serial mid-modiolar cross-sections were cut 4-μm thick, mounted on glass slides and counterstained with H&E. All slides were examined on an Olympus Optical (Tokyo, Japan) BX40 light microscope, and digital images were captured with the Olympus Optical DP70 camera.

T4 measurement

For serum preparation, trunk blood was collected from mutant and control mice by decapitation, whole blood was chilled on ice for 30 min and then spun at 10,000 rpm for 10 min in a benchtop centrifuge. Thyroxine (T4) was measured on a Beckman Synchron CX5 DELTA photometric chemistry analyzer (Beckman Coulter, Inc., Brea, CA) with the Synchron CX System, the associated T4 reagent (thyroxine kit, Beckman Coulter, Inc., Brea, CA), and the Synchron T4 calibrator. This system allows automated measurements of T4.

Morphological Examinations of Eyes

A Nikon biomicroscope (slit lamp) was used to examine the cornea for clarity, size (bupthalmos vs. microcornea), surface texture, and vascularization. The iris was checked for pupil size, constriction, reflected luminescence, and synechia. The eye was then dilated with 1 % atropine and the lens checked for cataracts. An indirect ophthalmoscope was used to examine the fundus for signs of retinal degeneration, such as retinal vessel constriction or retinal pigment epithelial disturbance, or for other problems, such as drusen or deposits or optic nerve head abnormalities.

ABR Assessment of Hearing

Hearing in mice was assessed by auditory brainstem response (ABR) threshold analysis. Mice were anes-

thetized with an intraperitoneal injection of tribromoethanol (0.2 ml of 20 mg/ml stock per 10 g of body weight), and then placed on a 37 °C temperature-controlled pad in a sound-attenuating chamber. Needle electrodes were placed just under the skin, with the active electrode placed between the ears just above the vertex of the skull, the ground electrode between the eyes, and the reference electrode underneath the left ear. High-frequency transducers were placed just inside the ear canal and computer-generated sound stimuli were presented at defined intervals. Thresholds were determined for broad-band clicks and 8-, 16-, and 32-kHz pure tone stimuli by increasing the sound pressure level in 10-dB increments followed by 5-dB increases and decreases to determine the lowest level at which a distinct ABR wave pattern could be recognized. Stimulus presentation and data acquisition were performed using the Smart EP evoked potential system (Intelligent Hearing Systems, Miami, FL).

Statistical Analyses

Statistical tests of body weights and ABR thresholds of mutant mice were performed using the JMP 10.0 interactive statistics and graphics software program (www.JMP.com). Statistical significance of the differences among means was determined by one-way and two-way ANOVA analyses with Tukey–Kramer HSD tests to correct for multiple pair-wise comparisons.

Genetic Mapping

To map the *tee* mutation, ovaries from homozygous mutant females were transferred to host females who then were mated with CAST/EiJ males. The resulting F1 hybrids were intercrossed and 21 mutant (dwarf) F2 progeny were produced and analyzed for linkage by their associations with microsatellite DNA markers typed by PCR amplification and agarose gel separation. Genomic DNA for genotyping mice was rapidly prepared from tail tips by the hot sodium hydroxide and Tris procedure (Truett et al. 2000). PCR reactions were comprised of 75 ng genomic DNA in 25 µl containing 500 mM KCl, 100 mM Tris–HCl (pH 8.3 at 25 °C), and 0.01 % Tritin-X-100, 15 mM $Mg(OAc)_2$, 100 nM of each primer (forward and reverse), 0.2 mM of each of four deoxyribonucleoside triphosphates, and 0.5 U of Taq DNA polymerase (5 Prime Inc., Gaithersburg, MD). PCR was run in a Bio-Rad Peltier thermal cycler. Amplification consisted of 1 cycle of denaturation at 97 °C for 30 s followed by 40 cycles, each consisting of 94 °C for 30 s (denaturation), 58 °C for 30 s (annealing), and 72 °C for 30+1 s (extension). After the 40 cycles, the final product was extended for 10 min at 72 °C. PCR products were visualized on 2.5 % NuSieve (Lonza Bioscience, Rockland, ME) agarose gels.

DNA Sequencing

PCR primers for amplifying portions of the mouse *Tpo* gene for mutant and control sequence comparisons were designed using Primer3 (http://primer3.sourceforge.net/) and synthesized by Integrated DNA Technologies (Coralville, IA). Primer sequences for genomic DNA and cDNA amplification are given in Table 1. To produce cDNA, total RNA was isolated from thyroid glands of mice at 4 weeks of age with the TRIzol reagent (Invitrogen Life Technologies, Carlsbad, CA), and the iScript cDNA synthesis kit (Bio-Rad Laboratories, Hercules, CA) was used to make first-strand cDNA. PCR products, either directly from reaction mixes or in some cases extracted from agarose gels, were purified with the QIAquick PCR purification kit (Qiagen Inc., Valencia, CA). Primers used for DNA amplification also were used for DNA sequencing on an Applied Biosystems 3700 DNA Sequencer with an optimized BigDye Terminator Cycle Sequencing method.

Genotyping

Mutant mice do not breed, and the strains originally were maintained by progeny testing or by ovary transplants to host females; however, molecular genotyping now allows direct identification of heterozygotes for simplified colony maintenance. To genotype the Tpo^{tee} mutation, PCR primers Tpo-teeF and Tpo-teeR (Table 1) were designed to amplify a 150 bp fragment of exon 11 of the *Tpo* gene, which contains the *tee* mutation site. After incubation with the restriction enzyme *Mse*I, the PCR product from uncleaved wild-type DNA is 150 bp, whereas the PCR product from mutant DNA is cleaved into 95 and 55 bp fragments. For restriction enzyme digestion, a 15-µL aliquot of each PCR-amplified DNA sample was mixed with 0.8 µL *Mse*I (New England Biolabs, Ipswich, MA) and incubated at 37 °C for 2–4 h. Each sample was then run on a 1.5 % SeaKem (Lonza Bioscience, Rockland, ME) agarose gel to resolve PCR product sizes. To genotype the $Tpo^{tee\text{-}2J}$ mutation, PCR primers TpoEx5-F and TpoEx5-R (Table 1) were used to amplify the exon 5 region of *Tpo*, which contains the site of the *tee-2J* deletion. The amplified fragment of wild-type DNA is 269 bp, whereas the amplified fragment of DNA with the *tee-2J* mutation is 205 bp. The 64-bp difference in the sizes of these fragments can easily be resolved by agarose gel electrophoresis.

TABLE 1

PCR primers used for *Tpo* mutation analyses

	Forward primer		*Reverse primer*			
Exon	*Name*	*Sequence*	*Name*	*Sequence*	*Product Size (bp)*	
PCR primers for sequencing *Tpo* genomic DNA, flanking exons					Wild-type	*tee-2J*
1	TpoEx1-F	AGGGAGATCAAGTCCCCAG	TpoEx1-R	TGCCCAATAATGGTCTCCC	206	
2	TpoEx2-F	GCCTGGGTATTTATGGTACATCC	TpoEx2-R	CATGTTTGGTTTGTTGAGTGTG	239	
3	TpoEx3-F	TCTGCCCTTGAGGAAGAAAG	TpoEx3-R	AATGCCTCAGTTGCAAAAGG	225	
4	TpoEx4-F	ACATTTGCAAACTGAGCTGC	TpoEx4-R	GAGCATGTTTAGCTGTTTCTCC	336	
5	TpoEx5-F	CTGGGAGGAAGAACCAACTG	TpoEx5-R	AGAGCCCACTTTGCAGTGAC	269	205
6	TpoEx6-F	TGTATTGAGACCTCAACATTTCTTC	TpoEx6-R	GGAGTCTTATAGCATTATGGAAAACC	265	
7	TpoEx7-F	TTATTGATCACGGGGCAGTC	TpoEx7-R	TTTGCATTTATGTTAAGCTTTTCTG	346	
8	TpoEx8-F	AAGATTCTAAAAGGGCACACG	TpoEx8-R	CACATCTTAGGAGCATCCAGG	617	
9	TpoEx9-F	ACCTACAGGTATCCCTGGGC	TpoEx9-R	AGGCTCAGGCTGGGCTAC	394	
10	TpoEx10-F	GAATCTATCCTGGGTTCCCC	TpoEx10-R	AGCCCGAGAGTTCTTCCTTC	304	
11	TpoEx11-F	GCTTCCAGGGGTCAGCAG	TpoEx11-R	GCCCTGTGTTATGCCCAG	378	
12	TpoEx12-F	CTCCATTGGGGTGTCAAG	TpoEx12-R	CTCTTTGAGAGGTTAAACTGACG	349	
13	TpoEx13-F	AGGGCTGGTGGTCTAGAGTC	TpoEx13-R	GATCTGATGTTTTCCACAGGG	310	
14	TpoEx14-F	ATGGAGCTGAGGACATGGG	TpoEx14-R	GAAAGTCTGAGAACCTCAAACAC	272	
15	TpoEx15-F	CAGGTGGGGACCTGTGG	TpoEx15-R	AGGGGAGCTTTGAGAAGAGC	235	
16	TpoEx16-F	GGCCCTGGAGTGGTCTTC	TpoEx16-R	CAGATGTAGAAGCAGCTGATAGTC	264	
17	TpoEx17-F	TACCGCAGTGACTTGAGTGG	TpoEx17-R	AGAGTGGGAAGACAAGGAAGG	689	
PCR primers for sequencing *Tpo* cDNA, within exons					Wild-type	*tee-2J*
1 to (7/8)	Tpo1F	ACCCAGCGGTGCACATCCTG	Tpo1R	GTTTGAGGGAAGCTGTATGG	873	740+588
7 to 10	Tpo2F	ACTGCCAGCTGACCTGTGAG	Tpo2R	AGGAGGCCTCTCACTATCGG	818	
9 to 14	Tpo3F	GACCCTGGAGGCTTATCCAG	Tpo3R	AGGTGGGTGTGTCAGATCTG	847	
13 to 17	Tpo4F	GACTCCGAACCTCCTGTCTG	Tpo4R	TCTGGCTCCAAAGCAGTGAG	444	
PCR primers for genotyping mutations					Wild-type	Mutant
tee missense mutation						
11	Tpo-teeF	TGAGCTGAACAAGGCCATTG	Tpo-teeR	ATGATACATGCAAACAGAGG	150	95+55
					after *Mse*I digestion	
tee-2J deletion mutation						
5	TpoEx5-F	CTGGGAGGAAGAACCAACTG	TpoEx5-R	AGAGCCCACTTTGCAGTGAC	269	205

RESULTS

Origins and Dwarf Phenotype of Mutant Mice

Mice carrying two new recessive mutations causing similar dwarf phenotypes were discovered in separate colonies at The Jackson Laboratory and named "teeny" (*tee*) and "teeny-2 Jackson" (*tee-2J*). The official designations for these mutations are Tpo^{tee} and $Tpo^{tee\text{-}2J}$, but for simplicity, they are referred to here as *tee* and *tee-2J*. The *tee* mutation occurred in progeny of C57BL/6J (B6) mice that had been treated with ethyl nitrosamine urea, and the *tee-2J* mutation occurred spontaneously in a congenic colony of B6 mice carrying the $H2^{g7}$ histocompatibility allele (strain B6.Cg-$Tpo^{tee\text{-}2J}$ $H2^{g7}$/J). A mating of a +/*tee-2J* female with a +/*tee* male produced three mutants out of a total of seven progeny in two litters. The mutant phenotype of *tee*/*tee-2J* compound heterozygotes (non-complementation) indicates that the recessive mutations are alleles of the same gene. Homozygous mutant mice (*tee*/*tee* and *tee-2J*/*tee-2J*) do not breed but live normal lifespans.

Mice homozygous for either mutation (abbreviated B6 *tee* and B6 *tee-2J*) can be characterized by 1 week of age by their small size in comparison with their littermates, and this small size continues throughout their lifespan (Fig. 1). Mutant mice of the derived C3.B6-$Tpo^{tee\text{-}2J}$ congenic strain (abbreviated C3H *tee-2J*) are also dwarf (Fig. 1A). At 6–7 weeks of age, mean weights were 7.9, 8.5, and 8.1 g for the B6 *tee* (N=8), B6 *tee-2J* (N=6), and C3H *tee-2J* (N=6) mutant mice, respectively. Results of a one-way ANOVA test ($F_{(2, 17)}$= 0.29, P=0.75) indicate that mean weights of these dwarf mutants are not significantly different. X-rays of three 10.5-week-old *tee* mutants showed that there was no abnormal shortening of the long bones compared with an age-matched control and confirmed that the normally proportioned mutants are ateliotic dwarfs. The femurs of all three mutants looked thicker than normal, were splayed at the distal end, and appeared to be undermineralized.

The thyroid glands of mutant mice are dysplastic with poorly developed follicles and hyperproliferation of epithelial cells (Fig. 2). These pathologies indicate a lack of thyroid hormone synthesis and consequent loss of feedback inhibition on thyrotropic hormone activity. At 5–8 weeks of age, serum levels of T4 in 11 B6 *tee* mutant mice (5 females and 6 males) and in 9 B6 *tee-2J* mutant mice (4 females and 5 males) were below detectable levels (<0.4 μg/dl) as compared to 12 +/*tee* heterozygous control mice (8 females, 4 males) that had normal levels of T4 (4.9–8.5 μg/dl), confirming that mutant mice are severely hypothyroid.

Eyes of two B6 *tee* mutant mice were carefully examined (see Methods), but structural abnormalities were not detected. The cornea, iris, lens, and retina appeared normal in all four mutant eyes examined.

Hearing Impairment and Cochlear Pathology of Mutant Mice

To assess hearing in mutant and control mice, we measured their ABR thresholds to broadband clicks and to 8, 16, and 32 kHz pure tone stimuli. Homozygous mutant mice (*tee*/*tee* and *tee-2J*/*tee-2J*) had highly elevated thresholds (60–70 dB hearing loss) for all four stimuli compared with age-matched non-mutant controls (Table 2, Fig. 3). To investigate the influence of genetic background on hearing in mutant mice, we compared the thresholds of *Tpo* mutant mice on a C57BL/6J background, strain C57BL/6J-Tpo^{tee} (B6 *tee*), and strain B6.Cg-$Tpo^{tee\text{-}2J}$

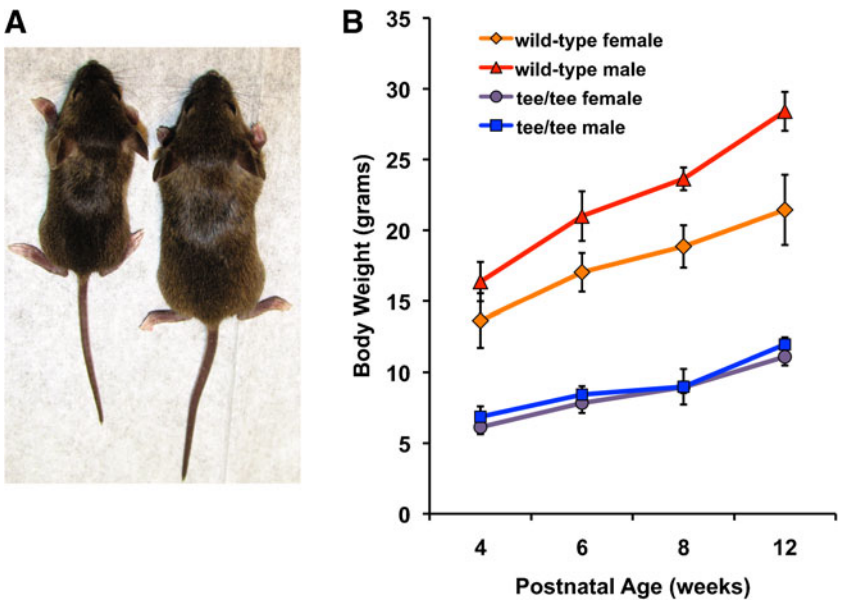

FIG. 1. The dwarf phenotype of mutant mice. The *tee*/*tee* and *tee-2J*/*tee-2J* mutant mice have the same dwarf appearance and reduced growth rates. **A** A normally proportioned (ateliotic) dwarf mouse (C3.B6-$Tpo^{tee\text{-}2J/tee\text{-}2J}$) compared with its wild-type littermate at 32 days of age. **B** Average body weights of female (N=5) and male (N=7) non-mutant littermate control mice (wild-type) compared with those of age-matched female (N=6) and male (N=6) C57BL/6J-$Tpo^{tee/tee}$ mutant mice (tee/tee) at 4, 6, 8, and 12 weeks of age. *Error bars* indicate standard deviations of the means.

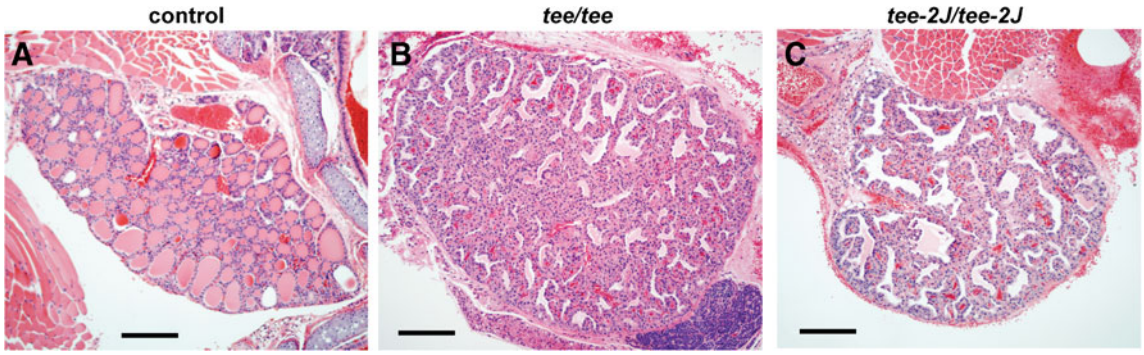

FIG. 2. Thyroid gland pathology of mutant mice. Cross-sections of thyroid glands stained with H&E from an 8-week-old +/+ control (**A**) and age-matched *tee/tee* (**B**) and *tee-2J/tee-2J* mutants (**C**). Thyroid glands of mutant mice lack normal follicles containing colloid material and have highly proliferating epithelial cells that give rise to adenomas (goiters). All *scale bars,* 200 μm.

$H2^{g7}$/J (B6 *tee-2J*), with those of *Tpo* mutant mice on a C3H/HeJ strain background, congenic strain C3.B6-$Tpo^{tee\text{-}2J}$ (C3H *tee-2J*). A one-way ANOVA test of broadband click responses and strain/genotypes (B6 *tee*, B6 *tee-2J*, and C3H *tee-2J*) showed a significant strain/genotype effect on thresholds ($F_{(2,\ 29)}$=4.63, P=0.018). The post hoc Tukey test detected statistically significant differences between mean click thresholds of B6 *tee* and C3H *tee-2J* mutant mice (P=0.0331) and between B6 *tee-2J* and C3H *tee-2J* mutant mice (P=0.0382) but no significant difference between B6 *tee* and B6 *tee-2J* mutant mice (P=1.000). For the pure tone frequency responses, a two-way ANOVA was performed for strain/genotype × stimulus frequency (8, 16, and 32 kHz). Both strain/genotype ($F_{(2,\ 91)}$=9.39, P=0.0002) and stimulus frequency ($F_{(2,91)}$=19.00, P<0.0001) effects were highly significant. For the strain/genotype effect, the Tukey test detected statistically significant differences between mean thresholds of B6 *tee* and C3H *tee-2J* mutant mice (P=0.0008)

TABLE 2

ABR thresholds of *Tpo* mutant and control mice on different strain backgrounds. Numbers of female (f) and male (m) mice tested, threshold means, standard deviations (S.D.), and standard errors (S.E.) are given for each genotype-strain combination. Data for males and females within each group were combined because no statistically significant differences were observed

				ABR thresholds (dB SPL)				
Tpo genotype	*Strain background*	*Number tested*	*Age in months*	*Click*	*8 kHz*	*16 kHz*	*32 kHz*	
+/+	C57BL/6J	5 f	3	41.8	34.7	16.6	45.0	Mean
		11 m		5.6	3.9	2.9	6.2	S.D.
				1.28	0.97	0.67	1.43	S.E.
+/+	C3H/HeJ	4 f	2.5	37.5	40.6	19.4	42.5	Mean
		4 m		3.8	4.2	1.8	4.6	S.D.
				1.34	1.48	0.63	1.64	S.E.
+/tee	C57BL/6J	1 f	1.5	36.7	40.0	20.0	40.0	Mean
		2 m		5.8	0.0	0.0	0.0	S.D.
				3.33	0.00	0.00	0.00	S.E.
+/tee-2J	C57BL/6J[a]	1 f	4	38.3	36.7	23.3	45.0	Mean
		2 m		2.9	2.9	5.8	0.0	S.D.
				1.67	1.67	3.33	0.00	S.E.
tee/tee	C57BL/6J	6 f	1.5	100.0	100.0	87.7	99.5	Mean
		5 m		0.0	0.0	6.1	1.5	S.D.
				0.00	0.00	1.93	0.05	S.E.
tee-2J/tee-2J	C57BL/6J[a]	4 f	1.5	100.0	99.0	88.0	100.0	Mean
		6 m		0.0	3.2	6.9	0.0	S.D.
				0.00	0.96	2.08	0.00	S.E.
tee-2J/tee-2J	C57BL/6J[a]	2 f	4	100.0	100.0	82.5	100.0	Mean
				0.0	0.0	3.54	0.0	S.D.
				0.00	0.96	2.50	0.00	S.E.
tee-2J/tee-2J	C3H/HeJ[b]	4 f	1.5	89.5	87.3	75.9	95.9	Mean
		7 m		15.7	18.8	19.0	9.7	S.D.
				4.74	5.66	5.70	2.92	S.E.

[a]Congenic strain B6.Cg-$Tpo^{tee\text{-}2J}$ $H2^{g7}$

[b]Congenic strain C3.B6-$Tpo^{tee\text{-}2J}$

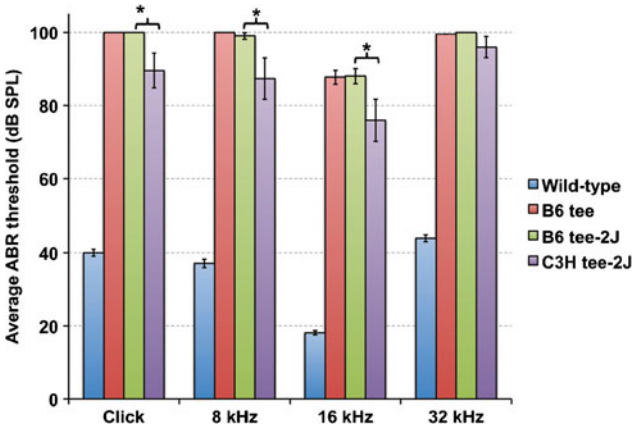

FIG. 3. Hearing impairment of mutant mice. Average ABR thresholds (with standard errors) are shown for broadband clicks and 8, 16, and 32 kHz pure tone stimuli for 30 non-mutant control mice (wild-type, *blue bars*), 11 *tee*/*tee* mutant mice of strain C57BL/6J-*Tpo*^{tee} (B6 tee, *red bars*), 10 *tee-2J*/*tee-2J* mutant mice of congenic strain B6.Cg-*Tpo*$^{tee-2J}$ *H2*^{g7}/J (B6 tee-2J, *green bars*), and 11 *tee-2J*/*tee-2J* mutant mice of congenic strain C3.B6-*Tpo*$^{tee-2J}$ (C3H tee-2J, *purple bars*). *Asterisks* indicate statistically significant differences ($P<0.05$) in ABR thresholds between *Tpo* mutants on B6 versus C3H strain backgrounds. All mutant mice were tested between 6 and 8 weeks of age, and the average age of control mice was 12 weeks of age.

and between B6 *tee-2J* and C3H *tee-2J* mutant mice ($P=0.0012$) but no significant difference between B6 *tee* and B6 *tee-2J* mutant mice ($P=0.9993$).

To identify the cochlear pathology responsible for the hearing impairment of mutant mice, we examined histological cross-sections at postnatal day 7 (P7), P14, and P28 (Fig. 4). Cochlear development in mutant mice was delayed compared to age-matched control mice. In the mutant cochlea at P7, the thickened tectorial membrane remains attached to large columnar epithelial cells; whereas in control mice, the thinner tectorial membrane has detached from the underlying epithelial cells, which have shortened and form the lining of a distinct inner sulcus. The developmental stage of the mutant cochlea at P14 resembles that of the immature control cochlea at P7, whereas the control cochlea at P14 is fully formed with a distinct tunnel of Corti (the fluid-filled space separating the pillar cells) and space of Nuel (the space between the outer pillar cell and the first outer hair cell), features still undeveloped in the P14 mutant cochlea. By 1 month of age, the development of the mutant cochlea has progressed to resemble a normal mature cochlea; however, the abnormally thickened tectorial membrane is retained (Fig. 4G, H).

Genetic Mapping and Molecular Characterization of the Mutations

To identify candidate genes for the allelic *tee* and *tee-2J* mutations, we determined the chromosomal location of the *tee* mutation by generating and analyzing a genetic linkage cross. A female CAST/EiJ mouse was mated to a C57BL/6J mutant (*tee*/*tee*) male. The F1 progeny from this cross were intercrossed and produced 21 F2 progeny with dwarf phenotypes that were selected for linkage analysis. A genome-wide linkage screen was performed by PCR genotyping analysis of segregating microsatellite markers distributed on all chromosomes. Linkage of *tee* was first detected with marker *D12Mit11* on chromosome (Chr) 12. The F2 DNA samples were then typed for 11 additional Chr 12 markers, and the best gene order placed the *tee* mutation between *D12Mit11* (GRCm38 position 19.8 Mb) and *D12Mit146* (33.2 Mb), and non-recombinant with *D12Mit185* (27.1 Mb), *D12Mit283* (26.9 Mb), *D12Mit136* (30.2 Mb), *D12Mit270* (31.7 Mb), and *D12Mit106* (32.2 Mb). The thyroid peroxidase gene (*Tpo*) is located at the 30.1 Mb position on Chr 12, consistent with our localization of the *tee* mutation. *Tpo* was considered a likely candidate gene for *tee* and *tee-2J* based on this genetic map position and its crucial function in thyroid hormone biosynthesis.

The *Tpo* gene is comprised of 17 exons that span about 78 kb on mouse Chr 12. The NCBI reference sequence for *Tpo* mRNA (NM_009417) is a 3291-nucleotide transcript, which encodes a 914 amino acid protein (NP_033443). We found DNA alterations in *Tpo* that underlie both the *tee* and the *tee-2J* mutations (Fig. 5). We designed four pairs of PCR primers (Table 1) to amplify overlapping fragments of mouse *Tpo* cDNA. Sequence analysis of *tee*/*tee* mutant mice showed a single-base substitution (T to A) at position 1913 (NM_009417). The mutation changes a codon for tyrosine (TAC) to a codon for asparagine (AAC) at position 614 of NP_033443, and is designated Y614N. The mutation occurs in exon 11 of the *Tpo* gene and creates a new TTAA *Mse I* restriction site (Fig. 5C) that is useful for genotyping (see Methods). The single base-pair *tee* mutation found in *Tpo* cDNA was confirmed by sequence analysis of PCR products amplified from genomic DNA of additional *tee*/*tee* mutant mice.

Sequence analysis of PCR-amplified genomic DNA from *tee-2J*/*tee-2J* mutant mice using primers flanking each of the 17 exons of the *Tpo* gene (Table 1) revealed that the *tee-2J* mutation is a 64-bp deletion comprising the last 35 bps of exon 5 and the first 29 bps of intron 5, which includes the 5' splice donor site (Fig. 5). PCR amplification of cDNA from *tee-2J*/*tee-2J* mutant mice with primers corresponding to exons 1 and 9 (primers Tpo-1F and Tpo-1R, Table 1) revealed two abnormally sized products (740 and 588 bp) rather than the expected 873-bp product. Sequence analysis revealed that the 740-bp PCR product corresponded to a transcript that skipped

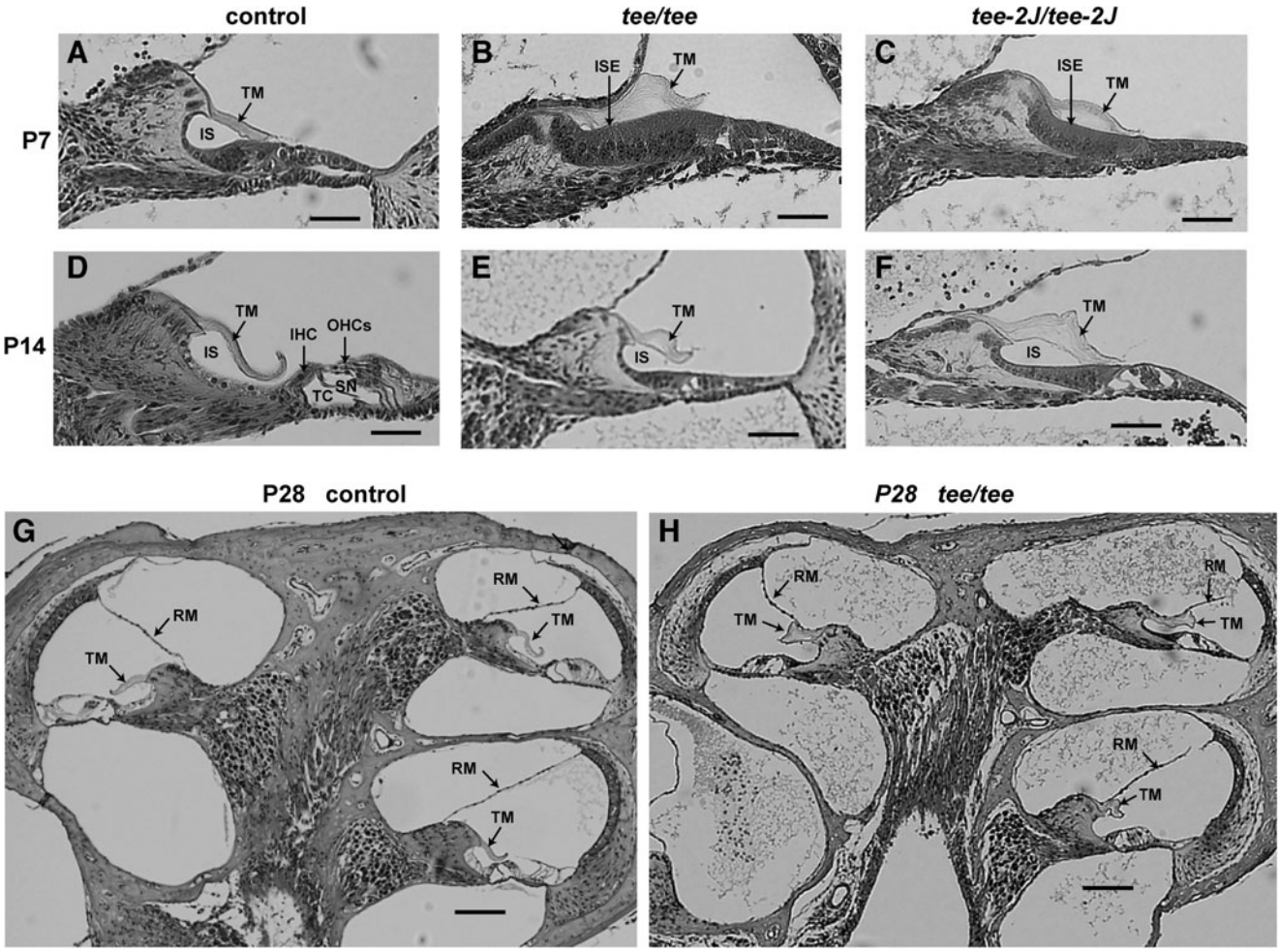

FIG. 4. Cochlear pathology of mutant mice. (**A**–**F**) Midmodiolar cross-sections through the middle turn of the cochlea focusing on the organ of Corti and spiral limbus in control (**A**, **D**), *tee/tee* mutant (**B**, **E**) and *tee-2J/tee-2J* mutant (**C**, **F**) mice at postnatal ages P7 (**A**–**C**) and P14 (**D**–**F**). In P7 mutants (**A**, **B**), the inner sulcus (*IS*) has not yet formed, and the inner sulcus epithelia (*ISE*) are still attached to a thickened tectorial membrane (*TM*). The developmental stage of the cochlea of mutant mice at P14 (**E**, **F**) resembles that of control mice at P7 (**A**): epithelial cells have shortened and detached from the tectorial membrane forming the inner sulcus. At P14, the tunnel of Corti (*TC*) and the space of Nuel (*SN*)—between the inner hair cell (*IHC*) and the outer hair cells (*OHCs*)—are fully formed in controls (**D**) but only beginning to form in mutants, which also retain a thickened tectorial membrane (**E**, **F**). (**G**-**H**) Midmodiolar cross-sections through the entire cochlea of a normal control and a *tee/tee* mutant mouse at adult age P28. In all cochlear turns, the tectorial membrane (*TM*) of mutant mice (**H**) retains an abnormally thickened appearance with partial attachment to Reissner's membrane (*RM*), not seen in age-matched controls (**G**). *Scale bars* in **A**–**F**, 50 μm. *Scale bars* in **G**-**H**, 100 μm.

only exon 5 (133-bp deletion) and that the 588-bp product corresponded to a transcript that skipped exons 4 and 5 (285-bp deletion). No normal transcripts were detected in cDNA from *tee-2J/tee-2J* mice. Skipping of exon 5 creates a frame shift that results in 12 incorrect amino acid substitutions (residues 111–122, NP_033443) followed by a premature stop codon. Skipping of exons 4 and 5 keeps the coding sequence in-frame but deletes 95 amino acids (residues 61–155, NP_033443).

DISCUSSION

Although hypothyroidism and dwarfing have previously been reported for a mouse mutation in *Tpo* (Takabayashi et al. 2006), we report here for the first time on the hearing impairment that is associated with mutations of this gene. The phenotypes of the two new *Tpo* mutations described here are very similar to the previously reported phenotype of the Tpo^{R479C} missense mutation (Takabayashi et al. 2006). The morphological abnormalities of the thyroid gland and the low T4 hormone levels caused by these *Tpo* mutations are characteristic of thyroid dyshormonogenesis. TPO is an essential enzyme in the synthesis of thyroid hormone and its iodide organification function is mediated by hydrogen peroxide. The NADPH-oxidase, DUOX2 has been shown to be the key provider of hydrogen peroxide in the thyroid gland (Moreno et al. 2003) and, as might

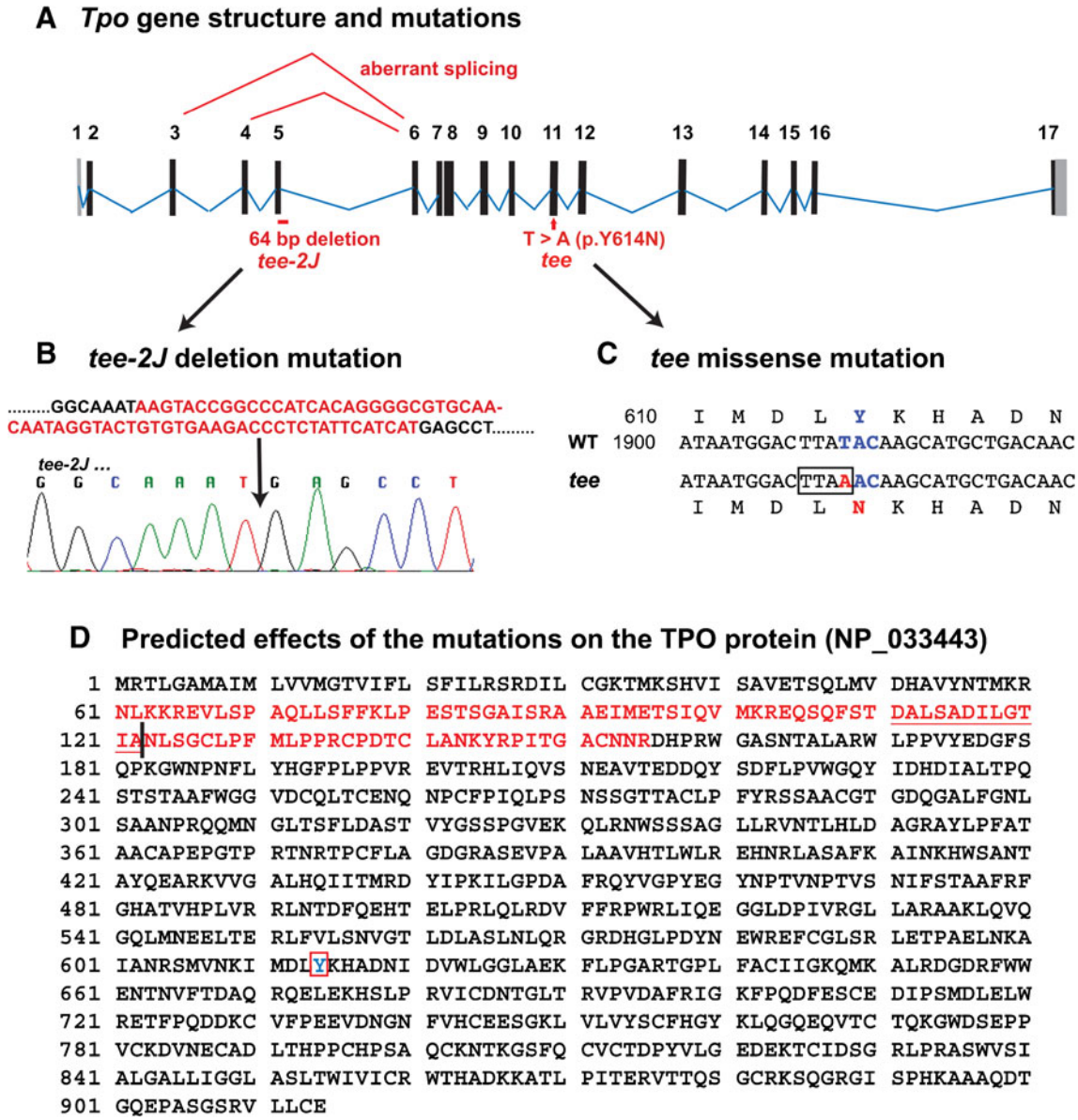

FIG. 5. Molecular characterization of the Tpo^{tee} and $Tpo^{tee\text{-}2J}$ mutations. **A** The mouse *Tpo* gene is comprised of 17 exons. Protein-coding exon regions are shown as *black vertical lines* and non-coding exon regions as *gray vertical lines*; introns are shown as *blue connecting lines*. The 64-bp deletion of the *tee-2J* mutation, which includes part of exon 5, and the single base-pair *tee* mutation in exon 11 are indicated in *red*. The aberrant exon 3–6 and exon 4–6 splicing patterns caused by inclusion of the intron 5 splice donor site in the *tee-2J* deletion are also shown in *red*. **B** DNA sequence chromatogram showing the position (indicated by *arrow*) of the 94 base pairs (in *red font*) that are deleted in the *tee-2J* mutation. **C** The T to A *tee* missense mutation is predicted to cause an amino acid change from tyrosine (*blue* Y, codon TAC) in the wild-type (*WT*) sequence to asparagine (*red* N, codon AAC) at residue 614 of the protein (p.Y614N). The boxed TTAA sequence in *tee* mutant DNA indicates the new *Mse*I restriction site created by the *tee* mutation. **D** Amino acid sequence of the TPO protein showing predicted effects of the mutations. The *tee-2J* deletion (*panel* **B**) causes aberrant splicing (*panel* **A**). Skipping of only exon 5 causes a frame shift that results in 12 incorrect amino acid substitutions (residues 111–122, *underlined*) before early termination (*vertical line*). If exons 4 and 5 are skipped, the coding sequence remains in-frame but 95 amino acids are deleted (residues 61–155, shown in *red*). The *tee* missense mutation changes the tyrosine (Y, shown in *blue* and *boxed in red*) at position 614 to asparagine.

be expected, the phenotype of mice deficient in DUOX2 (Johnson et al. 2007) is very similar to the phenotype of *Tpo* mutant mice.

The dysplastic thyroid glands, lack of detectable levels of T4, and severe dwarfing of mutant mice indicate that Tpo^{tee} and $Tpo^{tee\text{-}2J}$ are null mutations with no discernible TPO activity. The tyrosine (Y) at amino acid position 614 that is changed to asparagine (N) by the Tpo^{tee} mutation is highly conserved in all vertebrate species examined including *Xenopus* and zebrafish. The effect of the p.Y614N missense mutation on TPO protein function is predicted by the

PolyPhen-2 computer program (Adzhubei et al. 2010) to be probably damaging, with a score of 0.997, further supporting it as a functionally null mutation. The *Tpo*$^{tee\text{-}2J}$ mutation is also functionally null, causing aberrant splicing that prevents the formation of normal transcripts and protein.

The hearing impairment of the *Tpo* mutant mice is profound, with ABR thresholds 60–70 dB above those of non-mutant controls. Hearing impairment was detected in the youngest mutant mice tested (4 weeks) and does not progress. Thresholds for all frequency stimuli were equally affected. Genetic background is known to have significant effects on hearing phenotypes in mice (Johnson et al. 2006). In particular, the hearing loss associated with thyrotropin-deficient hypothyroid mice with mutations of the *Pou1f1* and *Prop1* genes is strongly influenced by strain background (Fang et al. 2011; Fang et al. 2012). ABR thresholds of mice with null mutations of *Pou1f1* are about 20 dB above normal on a C3H/HeJ strain background, whereas they are more than 70 dB above normal when on a C57BL/6J (B6) background (Fang et al. 2011). To investigate whether the hearing loss associated with hypothyroid *Tpo* mutant mice would be similarly modified by strain background effects, we produced a congenic C3.B6-*Tpo*$^{tee\text{-}2J}$ strain of mice to compare with the C57BL/6J-*Tpo*^{tee} and B6.Cg-*Tpo*$^{tee\text{-}2J}$ *H2*^{g7}/J strain mice. Thresholds of C3.B6-*Tpo*$^{tee\text{-}2J/tee\text{-}2J}$ mutant mice were indeed statistically significantly lower than *Tpo* mutant mice on the C57BL/6J strain background (Table 2, Fig. 3); however, the threshold difference attributable to the different strain backgrounds in *Tpo* mutant mice (10–12 dB) was less than that observed for *Pou1f1* mutant mice (~50 dB) when tested at 1.5 months of age. This result suggests that hearing-related factors in addition to hypothyroidism may be affected by the difference in strain backgrounds. The age-related hearing loss effect of the *Cdh23*^{ahl} variant of B6 mice is not likely accountable for the threshold difference because its effect on ABR thresholds is not detectable until mice are at least 3 months of age and is limited to high-frequency loss at that young age (Kane et al. 2012).

The delayed maturation of cochlear structures that we observed in *Tpo*^{tee} and *Tpo*$^{tee\text{-}2J}$ mutant mice, including delayed formation of the inner sulcus and tunnel of Corti, as well as a thickened and dysmorphic tectorial membrane, have been reported in other mouse models of congenital hypothyroidism (O'Malley et al. 1995; Li et al. 1999; Christ et al. 2004; Johnson et al. 2007) and in mouse models of resistance to TH (Rusch et al. 2001; Griffith et al. 2002; Ng et al. 2004). In addition to delaying cochlear development and causing malformations of the tectorial membrane, TH deficiency has been shown to affect the function of outer (Weber et al. 2002; Mustapha et al. 2009) and inner hair cells (Brandt et al. 2007; Sendin et al. 2007). Reduced or absent distortion product otoacoustic emissions have been observed in several different models of hypothyroid mutant mice (Li et al. 1999; Mustapha et al. 2009; Winter et al. 2009), suggesting that outer hair cell dysfunction may be a primary cause of TH-related hearing impairment. The ABR threshold shift of ~60 dB that we observed for *Tpo* mutant mice is similar to the hearing loss exhibited by mutant mice lacking outer hair cell electromotility (Liberman et al. 2002) and consistent with the idea that hypothyroid-associated hearing loss is the result of a defect in cochlear amplification (Song et al. 2008). It remains an open question, however, whether the tectorial membrane malformations observed in hypothyroid mice fully account for the loss of cochlear amplification.

TH regulates the expression of many genes and processes, and it is not clear which cochlear defects or combinations of defects are the major contributors to the hearing impairment associated with TH deficiencies (Mustapha et al. 2009). The *Tpo*^{tee} and *Tpo*$^{tee\text{-}2J}$ mutations we describe here provide new heritable mouse models for studies of congenital hypothyroidism and will be valuable tools for additional studies aimed at identifying the specific molecular mechanisms and pathologies that underlie TH-related hearing impairment.

ACKNOWLEDGMENTS

We thank Sandra Gray for mouse husbandry, blood collection, and ear dissections, Coleen Kane for thyroid gland preparations, and Rod Bronson for histology consultation. This work was supported by National Institutes of Health Grants R01 DC004301 (KRJ), R01 EY019943 (BC), P40 OD010972 (The Jackson Laboratory Mouse Mutant Resource), and P30 CA034196 (The Jackson Laboratory Shared Services).

REFERENCES

ADZHUBEI IA, SCHMIDT S, PESHKIN L, RAMENSKY VE, GERASIMOVA A, BORK P, KONDRASHOV AS, SUNYAEV SR (2010) A method and server for predicting damaging missense mutations. Nat Methods 7:248–249

AMBRUGGER P, STOEVA I, BIEBERMANN H, TORRESANI T, LEITNER C, GRUTERS A (2001) Novel mutations of the thyroid peroxidase gene in patients with permanent congenital hypothyroidism. Eur J Endocrinol 145:19–24

BAKKER B, BIKKER H, VULSMA T, DE RANDAMIE JS, WIEDIJK BM, DE VIJLDER JJ (2000) Two decades of screening for congenital hypothyroidism in The Netherlands: TPO gene mutations in total iodide organification defects (an update). J Clin Endocrinol Metab 85:3708–3712

Brandt N, Kuhn S, Munkner S, Braig C, Winter H, Blin N, Vonthein R, Knipper M, Engel J (2007) Thyroid hormone deficiency affects postnatal spiking activity and expression of Ca2+ and K+ channels in rodent inner hair cells. J Neurosci 27:3174–3186

Christ S, Biebel UW, Hoidis S, Friedrichsen S, Bauer K, Smolders JW (2004) Hearing loss in athyroid pax8 knockout mice and effects of thyroxine substitution. Audiol Neurootol 9:88–106

Deol MS (1973) Congenital deafness and hypothyroidism. Lancet 2:105–106

Everett LA, Belyantseva IA, Noben-Trauth K, Cantos R, Chen A, Thakkar SI, Hoogstraten-Miller SL, Kachar B, Wu DK, Green ED (2001) Targeted disruption of mouse Pds provides insight about the inner-ear defects encountered in Pendred syndrome. Hum Mol Genet 10:153–161

Fang Q, Longo-Guess C, Gagnon LH, Mortensen AH, Dolan DF, Camper SA, Johnson KR (2011) A modifier gene alleviates hypothyroidism-induced hearing impairment in pou1f1dw dwarf mice. Genetics 189:665–673

Fang Q, Giordimaina AM, Dolan DF, Camper SA, Mustapha M (2012) Genetic background of Prop1(df) mutants provides remarkable protection against hypothyroidism-induced hearing impairment. J Assoc Res Otolaryngol 13:173–184

Griffith AJ, Szymko YM, Kaneshige M, Quinonez RE, Kaneshige K, Heintz KA, Mastroianni MA, Kelley MW, Cheng SY (2002) Knock-in mouse model for resistance to thyroid hormone (RTH): an RTH mutation in the thyroid hormone receptor beta gene disrupts cochlear morphogenesis. J Assoc Res Otolaryngol 3:279–288

Johnson KR, Zheng QY, Noben-Trauth K (2006) Strain background effects and genetic modifiers of hearing in mice. Brain Res 1091:79–88

Johnson KR, Marden CC, Ward-Bailey P, Gagnon LH, Bronson RT, Donahue LR (2007) Congenital hypothyroidism, dwarfism, and hearing impairment caused by a missense mutation in the mouse dual oxidase 2 gene, duox2. Mol Endocrinol 21:1593–1602

Kane KL, Longo-Guess CM, Gagnon LH, Ding D, Salvi RJ, Johnson KR (2012) Genetic background effects on age-related hearing loss associated with Cdh23 variants in mice. Hear Res 283:80–88

Li D, Henley CM, O'Malley BW Jr (1999) Distortion product otoacoustic emissions and outer hair cell defects in the hyt/hyt mutant mouse. Hear Res 138:65–72

Liberman MC, Gao J, He DZ, Wu X, Jia S, Zuo J (2002) Prestin is required for electromotility of the outer hair cell and for the cochlear amplifier. Nature 419:300–304

Moreno JC, de Vijlder JJ, Vulsma T, Ris-Stalpers C (2003) Genetic basis of hypothyroidism: recent advances, gaps, and strategies for future research. Trends Endocrinol Metab 14:318–326

Mustapha M, Fang Q, Gong TW, Dolan DF, Raphael Y, Camper SA, Duncan RK (2009) Deafness and permanently reduced potassium channel gene expression and function in hypothyroid Pit1dw mutants. J Neurosci 29:1212–1223

Ng L, Goodyear RJ, Woods CA, Schneider MJ, Diamond E, Richardson GP, Kelley MW, Germain DL, Galton VA, Forrest D (2004) Hearing loss and retarded cochlear development in mice lacking type 2 iodothyronine deiodinase. Proc Natl Acad Sci U S A 101:3474–3479

Ng L, Hernandez A, He W, Ren T, Srinivas M, Ma M, Galton VA, St Germain DL, Forrest D (2008) A protective role for type 3 deiodinase, a thyroid hormone-inactivating enzyme, in cochlear development and auditory function. Endocrinology 150:1952–1960

O'Malley BW Jr, Li D, Turner DS (1995) Hearing loss and cochlear abnormalities in the congenital hypothyroid (hyt/hyt) mouse. Hear Res 88:181–189

Pfarr N, Borck G, Turk A, Napiontek U, Keilmann A, Muller-Forell W, Kopp P, Pohlenz J (2006) Goitrous congenital hypothyroidism and hearing impairment associated with mutations in the TPO and SLC26A4/PDS genes. J Clin Endocrinol Metab 91:2678–2681

Rusch A, Ng L, Goodyear R, Oliver D, Lisoukov I, Vennstrom B, Richardson G, Kelley MW, Forrest D (2001) Retardation of cochlear maturation and impaired hair cell function caused by deletion of all known thyroid hormone receptors. J Neurosci 21:9792–9800

Sendin G, Bulankina AV, Riedel D, Moser T (2007) Maturation of ribbon synapses in hair cells is driven by thyroid hormone. J Neurosci 27:3163–3173

Song L, McGee J, Walsh EJ (2008) The influence of thyroid hormone deficiency on the development of cochlear nonlinearities. J Assoc Res Otolaryngol 9:464–476

Sprenkle PM, McGee J, Bertoni JM, Walsh EJ (2001) Consequences of hypothyroidism on auditory system function in Tshr mutant (hyt) mice. J Assoc Res Otolaryngol 2:312–329

Takabayashi S, Umeki K, Yamamoto E, Suzuki T, Okayama A, Katoh H (2006) A novel hypothyroid dwarfism due to the missense mutation Arg479Cys of the thyroid peroxidase gene in the mouse. Mol Endocrinol 20:2584–2590

Truett GE, Heeger P, Mynatt RL, Truett AA, Walker JA, Warman ML (2000) Preparation of PCR-quality mouse genomic DNA with hot sodium hydroxide and tris (HotSHOT). Biotechniques 29(52):54

Uziel A (1986) Periods of sensitivity to thyroid hormone during the development of the organ of Corti. Acta Otolaryngol Suppl 429:23–27

Weber T, Zimmermann U, Winter H, Mack A, Kopschall I, Rohbock K, Zenner HP, Knipper M (2002) Thyroid hormone is a critical determinant for the regulation of the cochlear motor protein prestin. Proc Natl Acad Sci U S A 99:2901–2906

Winter H, Braig C, Zimmermann U, Geisler HS, Franzer JT, Weber T, Ley M, Engel J, Knirsch M, Bauer K, Christ S, Walsh EJ, McGee J, Kopschall I, Rohbock K, Knipper M (2006) Thyroid hormone receptors TRalpha1 and TRbeta differentially regulate gene expression of Kcnq4 and prestin during final differentiation of outer hair cells. J Cell Sci 119:2975–2984

Winter H, Ruttiger L, Muller M, Kuhn S, Brandt N, Zimmermann U, Hirt B, Bress A, Sausbier M, Conscience A, Flamant F, Tian Y, Zuo J, Pfister M, Ruth P, Lowenheim H, Samarut J, Engel J, Knipper M (2009) Deafness in TRbeta mutants is caused by malformation of the tectorial membrane. J Neurosci 29:2581–2587

Wu JY, Shu SG, Yang CF, Lee CC, Tsai FJ (2002) Mutation analysis of thyroid peroxidase gene in Chinese patients with total iodide organification defect: identification of five novel mutations. J Endocrinol 172:627–635